JOURNAL OF MATERIALS SCIENCE 13 (1978) 2462–2470

Dynamic observations of the fracture phenomena in alpha/beta brass two-phase bicrystals

NABIL FAT-HALLA*
Graduate School, Tohoku University, Sendai, Japan

TAKAYUKI TAKASUGI, OSAMU IZUMI
The Research Institute for Iron, Steel and Other Metals, Tohoku University, Sendai, Japan

In situ dynamic observations of the deformation and fracture characteristics of alpha/beta brass two-phase bicrystals were made by the solid diffusion method. The results indicated clearly that the crack initiation site was at the interface. The crack propagation direction, in both the alpha and beta phases, was found to be orientation dependent. Complementary experiments on alpha and beta brass single crystals confirmed the theories and results obtained previously on ductile single crystals.

1. Introduction

Two-phase alloys are extensively used in industry. The advantageous properties of α/β brass alloys such as good deformability, good machinability relatively high strength and moderate ductility have made this duplex alloy of special interest.

To further improve the existing properties of this alloy it is necessary to understand the fracture mechanism in order to combine high fracture strength with ductility and high resistance to shear. This would be complicated if such a study were carried out on a polycrystalline material, but the problem can be approached by considering the deformation and fracture behaviour of α/β brass two-phase bicrystals. Although a new technique for the preparation of bicrystals by the solid diffusion method has been reported recently [1], the authors preferred to use a modified method [2] which gave a nearly constant zinc concentration in both phases.

The present research was undertaken to clarify:

(i) The fracture origin (crack initiation site) in the two-phase bicrystal.

(ii) The crack propagation direction and its relation to orientation.

(iii) Deformation behaviour in both α- and β-phases, particularly near the interface.

(iv) The characteristics of the fracture surfaces.

2. Experimental procedure

High purity α- and β-brasses (trace elements <0.003 wt %) were used in obtaining single crystals of α-brass (29.6 wt % Zn) and β-brass (47.2 wt % Zn) using the Bridgman technique. The detailed procedure for the preparation of the bicrystals was described elsewhere [2]. A brief description is as follows: (i) The single crystal strips (2 mm × 10 mm × 30 mm) were ground on emery paper up to 800 mesh, and then electropolished in a solution of phosphoric acid, alcohol and distilled water; (ii) pairs of α- and β-single crystals were gently pressed into a graphite holder and after wrapping in copper foil were annealed at ~ 873 K for one week under an argon atmosphere. By this solid diffusion couple technique α/β brass bicrystals could be obtained having a newly grown β-layer about $0.7 \sim 1$ mm thick with an approximately constant zinc concentration. They also showed a straight phase interface [2]. The orientation relationship between the two phases was determined by the X-ray Laue method.

The scanning electron microscope (SEM) was chosen for this study owing to the unique properties of this apparatus [3]. In conjunction with the SEM a high performance video tape unit prepared for recording the dynamic fracture process was used. It allowed observations to be recorded on an

*On leave from the Mechanical Engineering Department, Al-Azhar University, Cairo, Egypt.

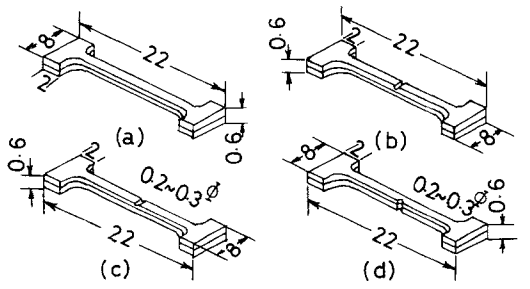

Figure 1 Dimensions and schematic illustration of the specimens: (a) unnotched bicrystal; (b) bicrystal notched in the α-phase; (c) bicrystal notched in the β-phase, and (d) bicrystal notched in both phases.

accurate time scale, and replays of the recorded images were possible at various speeds down to an image by image analysis.

Four types of tensile specimens were spark-machined to fit the tensile apparatus attached to the SEM. These types, together with their dimensions, are illustrated schematically in Fig. 1: (a) unnotched bicrystal; (b) bicrystal notched in the α-phase; (c) bicrystal notched in the β-phase; and (d) bicrystal notched in both phases.

All of the U-shape notches were spark-machined using a copper wire of 0.1 ~ 0.2 mm diameter. A tensile cross-head speed of 0.05 mm min^{-1} (initial strain rate of 5.9×10^{-5} sec^{-1}) was chosen to give reasonable rates of deformation and crack propagation.

The complementary tests on the α- and β-single crystals were performed on unnotched specimens of gauge length 18 mm and gauge cross-section of 3 mm × 0.7 mm. These specimens were deformed in tension up to fracture by an Instron-type machine; then the fracture surfaces were observed in the SEM in the hope of clarifying and supporting the results obtained with the bicrystals. All tests were conducted at room temperature.

3. Results

The initial observations were performed on the unnotched specimens, and since anticipation of the fractured region was therefore not always possible, it was preferred to notch the specimens so as to predetermine the fracture region. The specimens notched in the α-phase did not produce results any different from those observed for the unnotched specimens. It is believed that the high ductility of the α-phase eliminated the effect of stress concentrations under the notch, resulting in a flattened U-notch as deformation proceeded. Hence the results can be categorized into five groups as follows.

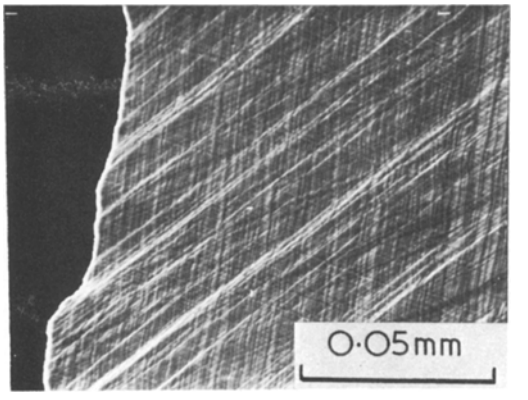

Figure 2 The edge of the fracture surface and neighbouring slip traces in the α-single crystal.

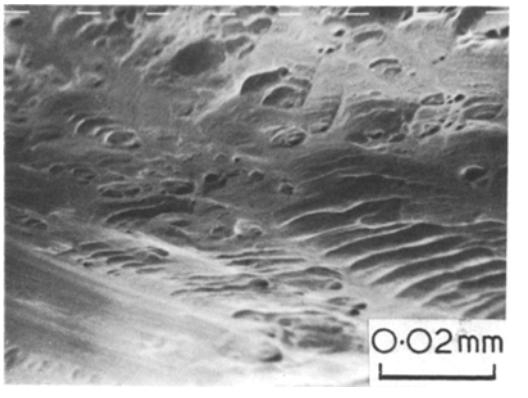

Figure 3 Smooth ripple pattern observed on the fracture surface of α-brass single crystals.

3.1. α-single crystals

Some α-single crystals with various orientations were deformed to fracture. Fig. 2 shows the edge of the fracture surface and the accompanying slip traces near the fracture region observed in one of these crystals. These slip planes activated near the fracture plane were determined as {1 1 1} planes by stereographic analysis.

Although severe "diffuse necking" occurred in the α-single crystals prior to fracture, resulting in a very narrow fractured surface, a rough determination of the fractured plane on a stereographic projection revealed its coincidence with one of the {1 1 1} slip planes.

A static observation of the fractured surfaces by the SEM showed a very smooth "ripple" pattern to be a dominant feature. This pattern occurs in

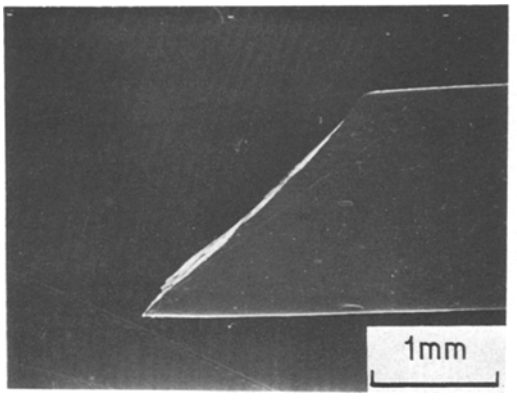

Figure 4 Slant fracture observed in β-single crystals together with faint slip traces.

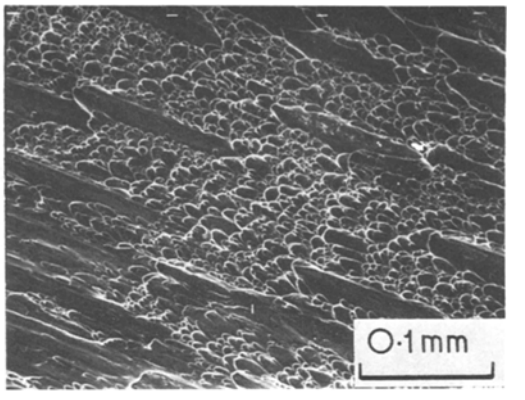

Figure 5 Typical elongated shear dimples on the fracture surface of β-single crystals.

the fracture of OFHC copper and some other metals [4]. A typical example of this smooth surface is given in Fig. 3.

3.2. β-single crystals

Most β-single crystals deformed on a single slip plane prior to fracture. This slip plane corresponded to {110}. Fig. 4 shows the edge of the fracture surface and the accompanying slip traces near the fractured region, as observed in one of the tested β-single crystals. No large amount of necking was observed in these crystals. The fractured planes usually corresponded to the primary slip planes within about ten degrees.

The dominant feature of the fractured surface was elongated shear dimples, as can be seen from Fig. 5. No inclusions could be observed within the dimples.

3.3. Unnotched bicrystals and bicrystals notched in the α-phase

Slip traces activated in the α-phase could easily be observed from the early stages of deformation, while those activated in the β-phase could not be seen clearly at moderate strains. In some specimens mechanical twinning occurred in the α-phase near the interface during deformation. "Shear steps"* (crack initiation site), whether propagated from the interface or nucleated in the interior of the β-phase, were observed in the necked region. These steps were halted at the interface in spite of the proceeding deformation (see Fig. 6) until localized shear bands penetrating into the α-phase formed at fronts of the steps, causing complete

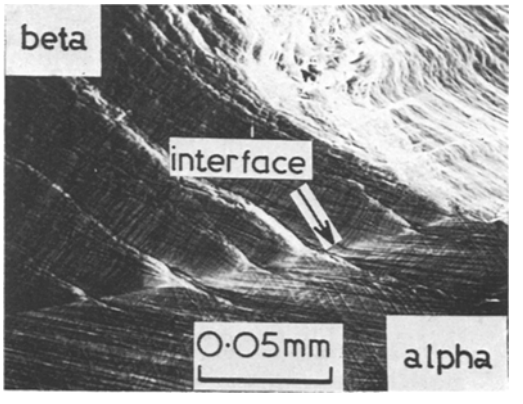

Figure 6 Shear steps halted at the interface.

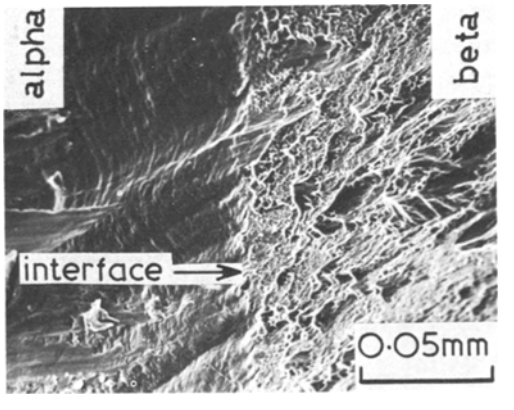

Figure 7 A typical pattern of the fracture surface observed in a two-phase bicrystal.

fracture of the specimen. It should be noted that no shear steps could be seen in the α-phase even after fracture.

An observation of the fractured surface in this

*We define this term as crack in which the two halves are separated by shear mode and thus formed a step on the free surface. Consequently, this term is different from "localized shear band" or "heavy plastic deformation".

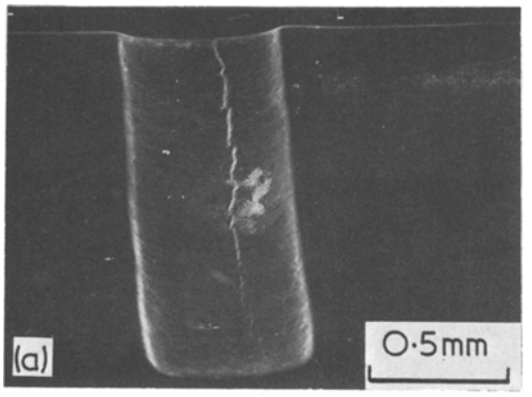

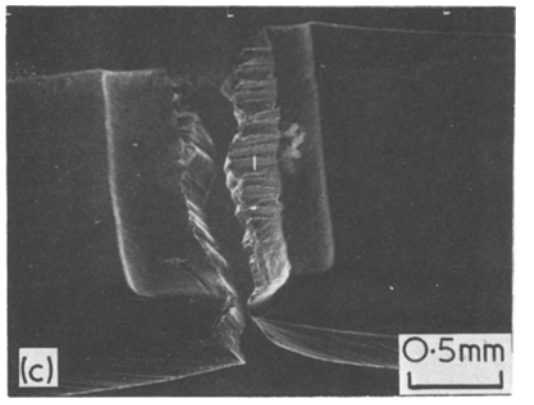

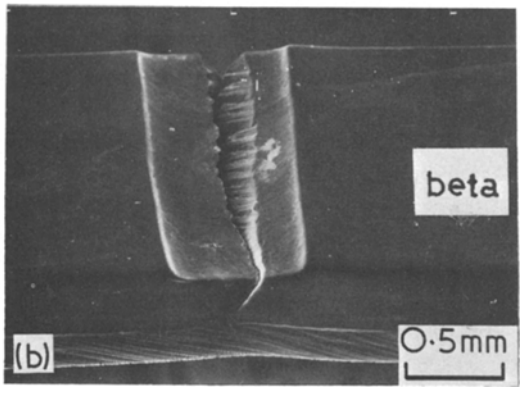

Figure 8 (a) Shear step at the root of a U-notch in a specimen notched in the β-phase. (b) Static photomicrograph showing the formation of a new shear step in the specimen shown in (a), and (c) change of the propagation direction in the same specimen.

type of specimen confirmed the results obtained previously [2]. Fig. 7 shows the typical dimple pattern in the β-phase and the smooth "ripple" pattern in the α-phase. Note that the ripples are parallel to each other and that they are nearly parallel to the interface. Thus, this type of bicrystal shows the transgranular shear type of fracture mode both macroscopically and microscopically.

3.4. Bicrystals notched in the β-phase

The elongation to fracture in these specimens was, as expected, lower than the former type of specimen due to the existence of the notch in β-phase. At strains near to that of fracture, a shear step developed almost parallel to the centre line of the notch root. A typical example is shown in Fig. 8a. Fig. 8b shows a static photograph of the propagation of the step as observed by SEM. The shear step propagated from the notch root toward the interface, but a new shear step having a different propagation direction was generated at the interface before the first shear step arrived there. Fracture was then completed by the propagation of the new step. This sequence is clearly seen at low magnification in Fig. 8c. A series of micro-

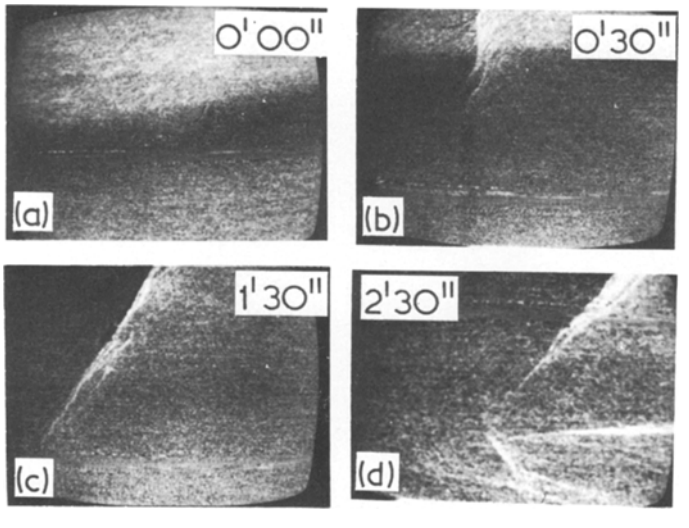

Figure 9 Sequence of photomicrographs showing the propagation of a shear step and the nucleation of a new shear step in the specimen shown in Fig. 8, as taken from replays of the recorded tape.

graphs taken from the video recording of the propagation of this shear step is shown in Fig. 9. A different development of the shear step on the notch root was observed. In this case a shear step inclined to the notch axis appeared at first, but the another shear step parallel to the notch axis dominated as the deformation proceeded. This second shear step propagated toward the interface, resulting in fracture of the specimen. The pattern on the fracture surfaces had the features of Fig. 7.

3.5. Bicrystals notched in both phases

The elongation to fracture was remarkably reduced in specimens notched in both phases. Also, the preferential fracture origin was at the interface, as can be seen from Fig. 10.

The examples shown in Figs. 10 and 11 illustrate (i) specimens in which the shear step direction in the β-phase is inclined to that in the α-phase, and (ii) specimens in which the shear step propagates in nearly the same direction in both phases. Thus different propagation behaviour of the shear step was observed.

The fracture surfaces in these specimens showed the common features observed in the last two types, i.e. the β-phase showed the shear dimple pattern and the α-phase the smooth ripple pattern.

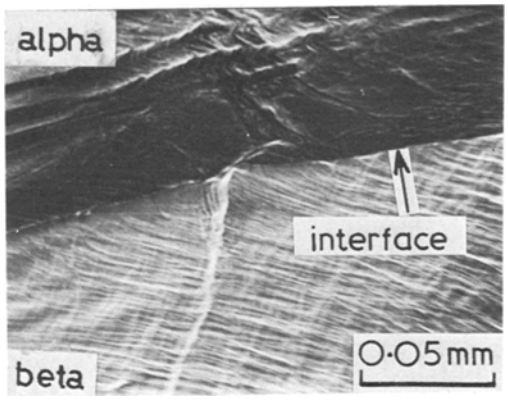

Figure 10 One of the specimens notched in both phases showing the propagation direction in both phases.

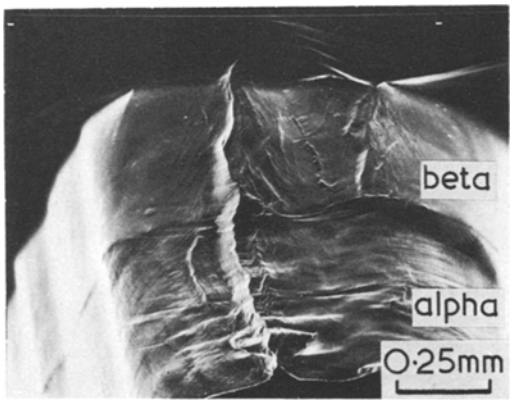

Figure 11 Bicrystal notched in both phases showing the same step propagation direction in both phases.

4. Discussion

4.1. α- and β-single crystals

It is well known [5] that shear fracture which occurs by the shearing of atomic bonds is actually a process of extremely localized (inhomogeneous) plastic deformation. Shear fracture in pure single crystals occurs when the two halves of the crystal slip apart on the crystallographic glide planes that have the greatest amounts of resolved shear stress. When the shear occurs on only one set of parallel planes a slant fracture is formed, while knife-edge or chisel-point fracture occurs when the shear takes place in two directions. Consistent with this criterion the results for the α- and β-single crystals showed slant fracture (see Fig. 12 and 4 respectively). The severe "diffuse necking" that was observed in the narrow face of the α-crystals is attributed not only to the activation of two slip systems prior to fracture but to the high ductility of this α-brass single crystal.

Taking into account the state of stress in the sheet tensile specimens used in the present work, Orwan [6], Spretnack [7] and Ghosh [8] have shown that this shape of specimens results in a "plane stress" conditon. Hence it is believed that the triaxial stress in the α-necked region was not sufficient to form voids; in other words the smooth

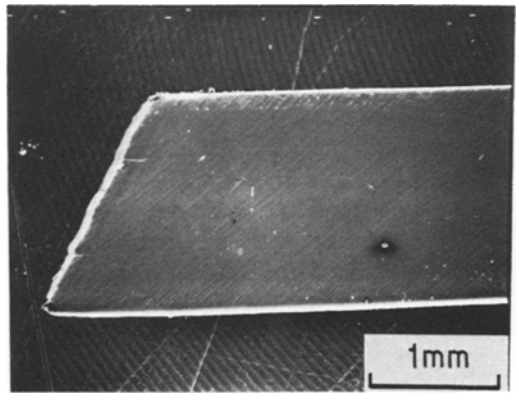

Figure 12 Slant fracture in the α-brass single crystal.

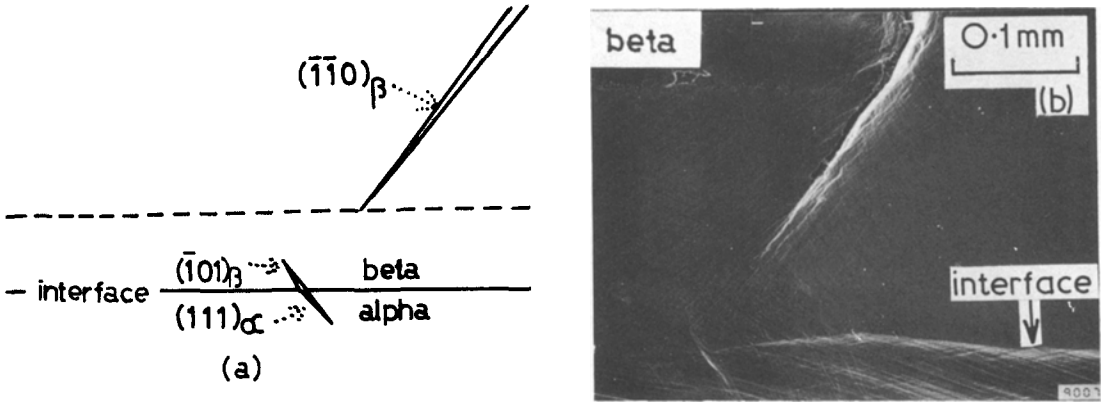

Figure 13 (a) Schematic illustration of crack propagation directions in the β- and α-phases in a specimen notched in the β-phase. (b) The specimen as viewed in SEM.

pattern observed on the fracture surface is attributed to (i) the lack of triaxial stress and (ii) the hgih purity of the materials used. Fracture of this type indicates a dominating "pure shear" process resulting in a featureless glide plane decohesion surface as was reported by Beachem [9] and Rogers [4], who observed the smooth ripple pattern in some ductile fcc metals. Moreover French *et al.* [10] observed this smooth pattern of shear fracture for α-brass and copper in the form of sheet tensile specimens. Thus, the remarkable necking and the resulting smooth pattern on the fracture surface of α-single crystal is attributed to its high ductility and the shape effect.

The deformation of β-single crystals prior to fracture showed localized shear deformation bands on which slant fracture occurred. Fracture coincided with the slip plane, as was pointed out earlier, and was in good agreement with the literature on β-single crystals [11, 12]. The nucleation voids in the absence of inclusions has been the subject of many studies; for instance Wilsdorf [13] studied the nucleation of these voids in silver single crystals, and Maclean [14] reviewed many possible models for the formation of these voids. However, regardless of the details of void formation on the atomic level (vacancy accumulation or dislocation interaction), microvoids could not be detected in regions at small distances from the fracture surface, indicating that the formation, growth and coalescence of the voids occurred at or very near to the fracture surface, i.e. in the highly localized deformed zone. Aside from the question of the void introduction, it is noted that the formation of the dimple pattern resulted from the low ductility of the β-crystal in comparison to that of the α-crystal.

4.2. Alpha/beta two-phase bicrystal

The orientations determined in regions near the fracture surfaces of the specimens, together with detailed photographs, were analysed on a stereographic projection. For simplicity the stereographic projection of the undeformed specimens will be referred to within this paper.

One of the specimens notched in β-phase revealed a change in the direction of shear step propagation, as can be seen in Figs. 13a and b. The first shear step propagated from the notch root was on the $(\bar{1}\,\bar{1}0)_\beta$ plane (see Fig. 14). Although this plane had a high value of resolved shear stress (RSS) it was not the primary slip plane. This behaviour reflects the complexity of the stress under the notch root. Just before the step (crack) front reached the interface, a new step having a different propagation direction was nucleated at the interface. An analysis of this new direction showed that it coincided with the matching planes* $(\bar{1}01)_\beta$ and $(1\,1\,1)_\alpha$ which both showed a high value of RSS. It is believed that the complex stress under the root of the notch resulted in the appearance of the first step $(\bar{1}\,\bar{1}0)_\beta$, and since there was no α-slip plane on the extension of the $(\bar{1}\,\bar{1}0)_\beta$ (see Fig. 14) the step had to alter its direction to that of the matching planes in both the α- and β-phases.

*The present bicrystal made by the solid diffusion couple method satisfied the orientation relationship of $\{1\,1\,1\}_\alpha \parallel \{1\,1\,0\}_\beta$ at the interface to within a few degrees. Consequently these planes are approximately coplanar.

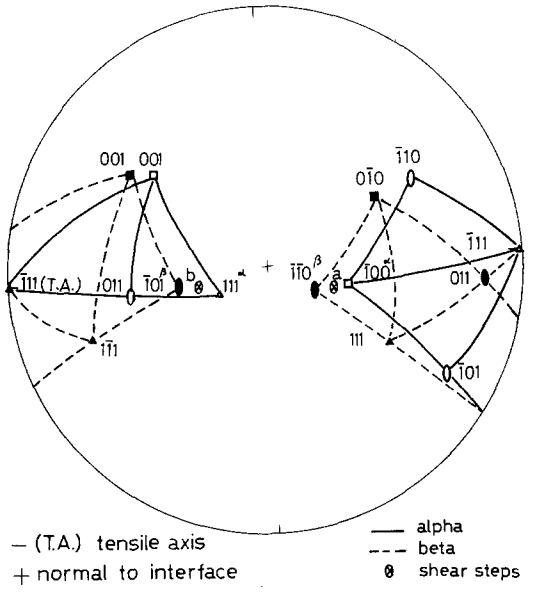

Figure 14 Stereographic projection of the specimen shown in Fig. 8 illustrating the change in crack direction from $(\bar{1}\bar{1}0)_\beta$ to the matching planes $(\bar{1}01)_\beta$ and $(111)_\alpha$:

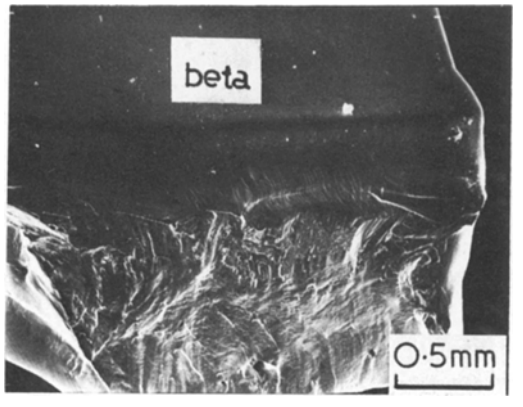

Figure 15 Illustration of the coincidence of the fractured planes in both the α- and β-phases in a specimen notched in the β-phase.

Now we can explain the fracture behaviour of the specimen which had an initial bias shear step on the notch root as follows: Although the stress state in the early stages of deformation produced this bias shear step, it showed high resistance to propagation into the whole matrix, restricted by the geometry. Therefore a new shear step which had a relatively high RSS and was parallel to the notch axis (minimum cross-section) was introduced. Moreoever, it should be emphasized that in this specimen the propagation on nearly coincident planes in both phases started at the interface, as can be seen in Fig. 15. That the shear step at the

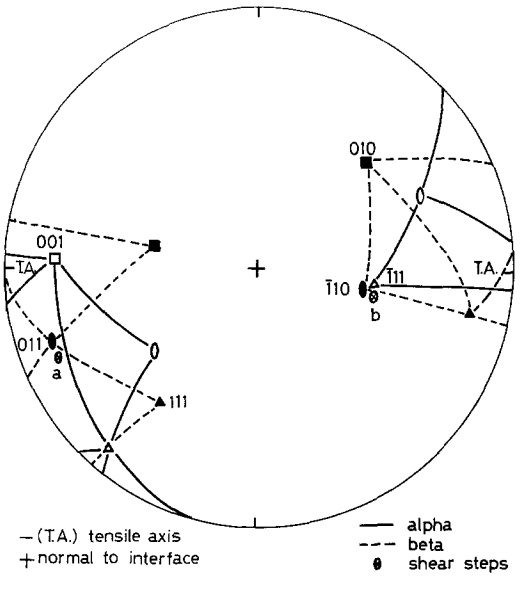

Figure 16 Stereographic analysis showing the change in shear step direction from the $(011)_\beta$ plane to the $(\bar{1}10)_\beta$ and $(\bar{1}11)_\alpha$ matching planes.

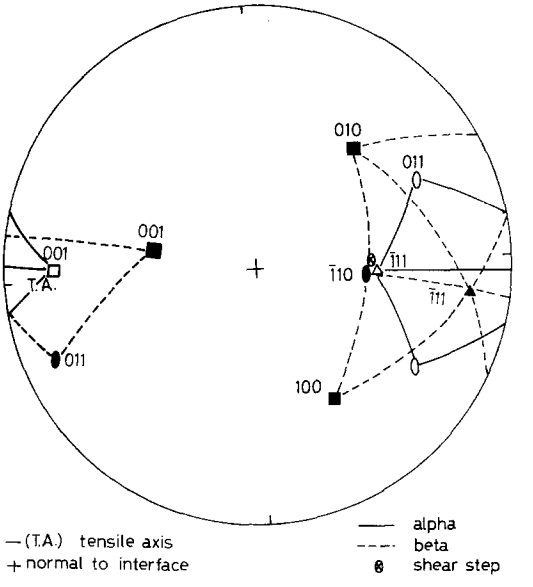

Figure 17 Stereographic projection showing clearly the coincidence of the crack propagation direction with the matching planes. Note that no change in propagation direction occurred. This diagram corresponds to Fig. 11.

root of the notch was parallel to the centre line supports the predictions given previously by Spretnack *et al.* [15], who concluded from finite element computer calculations that the expected crack must be away from the centre line but parallel to it.

In the case of specimens notched in both phases, the crack was found to nucleate at or very near to

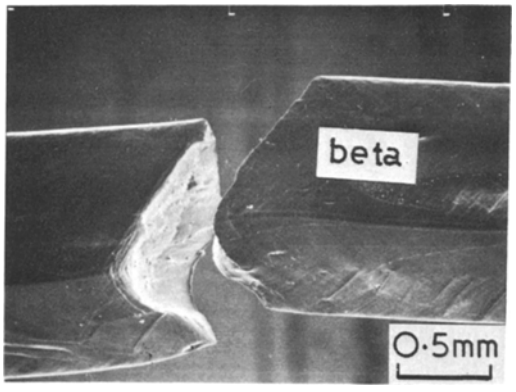

Figure 18 SEM macrograph showing a fracture plane passing through both β- and α-phases in an unnotched specimen.

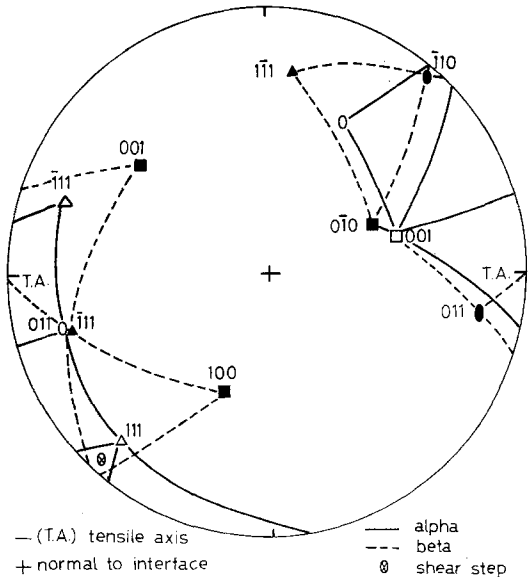

Figure 19 Stereographic analysis of the specimen shown in Fig. 18 showing the coincidence of the fracture plane with the matching planes.

interface. For instance, the specimen observed in Fig. 10 showed that out of twelve possible slip systems in the β-phase the step nucleated on the $(0\,1\,1)_\beta$ plane (see Fig. 16). Again this was not the primary slip plane, reflecting the complexity of stress under the notch root. The propagation of the crack into the α-phase then changed to $(\bar{1}\,1\,0)_\alpha$, which nearly coincided with the $(\bar{1}\,1\,0)_\beta$. The specimen shown in Fig. 11 demonstrates the case in which the shear step nucleated at the interface and propagated in both β- and α- phases in the same direction $[(\bar{1}\,1\,0)_\beta$ and $(\bar{1}\,1\,1)_\alpha]$, as illustrated in Fig. 17. Again these results can be interpreted with the aid of Figs. 16 and 17. It should be noted that the stress under the notch root depends on various factors, e.g. the interaction of the induced stress under the notch with the incompatible stress at the interface. Another factor arises depending on the exact geometry of the notch (e.g. notch width, depth and surface smoothness) which affects the stress to some extent. Hence, it is believed that the shear steps which were not on primary slip planes were caused by a complex stress state. Since no α-slip plane $\{1\,1\,1\}_\alpha$ existed in front of the shear step $(0\,1\,1)_\beta$ (see Fig. 16) the propagation direction was altered to that of $(\bar{1}\,1\,0)_\beta$ and $(\bar{1}\,1\,1)_\alpha$ (coinciding with each other). In the light of the above explanation the results can now be interpreted. The shear step near the interface was originally nucleated on $(\bar{1}\,\bar{1}\,0)_\beta$, and underwent no change in direction when propagating along $(\bar{1}\,1\,1)_\alpha$, as this was coplanar with $(\bar{1}\,\bar{1}\,0)_\beta$.

In the case of unnotched specimens it is clear that less complex stresses exist than in the notched specimens. Hence in this case all specimens clearly showed the nucleation of the shear step at the interface in the direction of the matching planes. For instance Fig. 18 shows one of these specimens in which the step propagation direction coincided (within experimental error) with the matching planes (see Fig. 19), on which the fracture occurred.

Hirth [16] reported that four independent sources of plastic strain are required to fix the variables at the interface in bicrystals, and he concluded that for bicrystals the plastic deformation of the crystals at the interface is relevant. Hence the present results indicating the initiation of cracks at the interface can be attributed to the plastic incompatibility conditions generated near the interface.

5. Conclusions

The following conclusions can be drawn from the results obtained in this research.

(1) A slant fracture plane was obtained, coinciding with the slip plane active prior to fracture in the α- and β-single crystals. This confirms pre-existing theories and results for the fracture of ductile single crystals.

(2) The crack propagation direction was found to be orientation dependent. The generation and propagation behaviour of the crack at the interface revealed the tendency to run on closely related planes in both phases.

(3) The fracture origin (crack initiation site) in two-phase bicrystals was found to initiate from the interface.

(4) The micro-features of the fracture surfaces were commmon to all types of bicrystals; the β-phase showed shear elongated dimples while the α-phase showed a smooth ripple pattern which was believed to be due to a pure shear process.

References

1. A. EBERHARDT, M. SUERY and B. BAUDELET, *Scripta Met.* **9** (1975) 1231.
2. T. TAKASUGI, N. FAT-HALLA and O. IZUMI, *J. Mater. Sci* **13** (1978) 2013.
3. J. FELLOWS, "Metals Handbook", Vol. 9 (American Scociety for Metals, Ohio, 1974) p. 49.
4. H. ROGERS, *Acta Met.* 7 (1959) 750.
5. A. TETELMAN and A. McEVILY, "Fracture of Structural Materials", 1st edn (John Wiley & Sons Inc., New York, London, Sydney, 1967) p. 38.
6. E. ORWAN, "Reports on Progress in Physics", 1st edn (The Physical Society, London 1949) p. 185.
7. A. CHAKRABARTI and J. SPRETNACK, *Met. Trans.* **6A** (1975) 733.
8. A. GHOSH, *ibid.* **8A** (1977) 1221.
9. C. BEACHEM, *Trans. ASM* **56** (1963) 318.
10. I. FRENCH, *Acta Met.* **24** (1976) 317.
11. S. HANADA, M. MOHRI and IZUMI, *Trans. Japan. Inst. Metals* (1975) **16** 453.
12. M. YAMAGUCHI and UMAKOSHI, *Acta Met.* **24** (1976) 1061.
13. L. LYLES and H. G. F. WILSDORF, *ibid.* **23** (1975) 269.
14. D. MACLEAN, "Mechanical Properties of Metals", 1st edn (John Wiley & Sons Inc., New York, London, 1962) p. 223.
15. V. RUSSO, A. CHAKRABARTI and J. SPRETNACK, *Met. Trans.* **8A** (1977) 729.
16. J. HIRTH, *Met. Trans.* **3** (1972) 3047.

Received 31 January and accepted 3 March 1978.